THE JOURNAL OF BIOLOGICAL CHEMISTRY VOL. 286, NO. 41, pp. 36142–36151, October 14, 2011

Swapping Small Ubiquitin-like Modifier (SUMO) Isoform Specificity of SUMO Proteases SENP6 and SENP7*[S]

Received for publication, June 6, 2011, and in revised form, August 24, 2011 Published, JBC Papers in Press, August 30, 2011, DOI 10.1074/jbc.M111.268847

Kamela O. Alegre[1] **and David Reverter**[2]

From the Departament de Bioquimica i Biologia Molecular, Institut de Biotecnologia i de Biomedicina, Universitat Autonoma de Barcelona, 08193 Barcelona, Spain

Background: The SENP/ULP family of SUMO proteases display different cleavage preference for SUMO isoforms.
Results: Insights into the structural determinants for the preference of SENP6 and SENP7 for the SUMO2/3 isoform.
Conclusion: A novel interface between SENP6 or SENP7 and SUMO determines the SUMO isoform preference.
Significance: This may be the first time that the cleavage preference between SUMO1 and SUMO2/3 was swapped by single point mutagenesis.

SUMO proteases can regulate the amounts of SUMO-conjugated proteins in the cell by cleaving off the isopeptidic bond between SUMO and the target protein. Of the six members that constitute the human SENP/ULP protease family, SENP6 and SENP7 are the most divergent members in their conserved catalytic domain. The SENP6 and SENP7 subclass displays a clear proteolytic cleavage preference for SUMO2/3 isoforms. To investigate the structural determinants for such isoform specificity, we have identified a unique sequence insertion in the SENP6 and SENP7 subclass that is essential for their proteolytic activity and that forms a more extensive interface with SUMO during the proteolytic reaction. Furthermore, we have identified a region in the SUMO surface determinant for the SUMO2/3 isoform specificity of SENP6 and SENP7. Double point amino acid mutagenesis on the SUMO surface allows us to swap the specificity of SENP6 and SENP7 between the two SUMO isoforms. Structure-based comparisons combined with biochemical and mutagenesis analysis have revealed Loop 1 insertion in SENP6 and SENP7 as a platform to discriminate between SUMO1 and SUMO2/3 isoforms in this subclass of the SUMO protease family.

The small ubiquitin-like modifier (SUMO)[3] belongs to the Ubl (ubiquitin-like) protein family, which is attached to protein substrates via an isopeptidic bond between their C-terminal glycine and a lysine residue on the substrate (1). After ubiquitin, SUMO is the second best characterized member of the Ubl family (2). SUMO is attached to target proteins by an enzymatic cascade analogous to ubiquitin (3). The SUMO pathway comprises a cascade of three enzymatic steps that leads to the formation of the isopeptidic bond on the target protein (4). The process can be reversed by the action of the SUMO proteases, which cleave off SUMO from the target protein. Thus, the abundance of SUMO substrates in the cell is regulated by a balance of conjugation by the SUMO enzymatic cascade and deconjugation by the SENP/ULP protease family (5).

The human SUMO protein family consists of four members, SUMO1, SUMO2, SUMO3, and SUMO4. SUMO4 does not seem to participate in the formation of SUMO conjugates *in vivo* (6). After maturation of their C-terminal tail, SUMO2 and SUMO3 are 95% identical (thus referred as SUMO2/3 in the text), whereas SUMO1 shares only 43% identity to SUMO2 or SUMO3. Recent reports indicate that SUMO isoforms are non-redundant in the cell; some substrates can be exclusively modified by SUMO1 or SUMO2/3, whereas others can be modified by both SUMO isoforms (7–9). Interestingly, *in vivo* heat shock or oxidative stress experiments produce an accumulation of SUMO2/3 in the cell, whereas SUMO1 remains unaltered (10). Another important difference between both SUMO isoforms is that SUMO2/3 can form polySUMO2/3 chains through an N-terminal lysine residue (11–13). One function of the polySUMO2/3 chains might be the stabilization of PML nuclear bodies (14), which is also the signal for the ubiquitin-dependent degradation by the recruitment of the E3 ubiquitin ligase RNF4 (15, 16). A recent study has analyzed the dynamics of conjugation/deconjugation of polySUMO chains, highlighting in *Schizosaccharomyces pombe* the role of deconjugation for the correct homeostasis of the cell (17).

In humans, the SENP/ULP protease family is comprised of seven members; six are SUMO-specific proteases (SENP1, SENP2, SENP3, SENP5, SENP6, and SENP7), whereas one is specific for another ubiquitin-like protein, Nedd8 (SENP8, also named DEN1 or NEDP1) (5). All SENPs share a conserved C-terminal domain of ~220 amino acid residues, containing the catalytic triad (His-Asp-Cys) characteristic of the cysteinyl proteases. Several crystal structures have been reported for the catalytic domains of some members of the family, in the apo form or in complex with SUMO substrates (18–23). All structures of the catalytic domains reveal a similar three-dimensional structure with conserved elements required for the correct proteolytic activity. Two different proteolytic activities can be performed by the SENP/ULP protease family, maturation of the SUMO precursor (processing) and hydrolysis of the isopep-

* This work was supported by Ministerio de Educacion y Ciencia Grant BFU2008-0364 and European Community Grant MIRG-CT-2007-200346.
[S] The on-line version of this article (available at http://www.jbc.org) contains supplemental Figs. 1 and 2.
[1] Supported by a scholarship from the Ministerio de Educacion y Ciencia.
[2] To whom correspondence should be addressed: Universitat Autonoma de Barcelona, 08193 Bellaterra, Barcelona, Spain. Tel.: 93-5868955; Fax: 93-581-2011; E-mail: david.reverter@uab.cat.
[3] The abbreviation used is: SUMO, small ubiquitin-like modifier.

tidic bond (deconjugation). Structural and functional analysis has revealed a preferential cleavage of the isopeptidic bond over the cleavage of the peptidic bond in deconjugation and processing reactions, respectively (24). Recent studies indicate that the members of the SENP/ULP family show preferential roles in the cleavage of SUMO substrates. For example, SENP2 exhibits a clear SUMO isoform preference in the processing reaction depending on the SUMO C-terminal tail, but the deconjugation reaction is faster and does not discriminate between SUMO1 and SUMO2/3 substrates (19). SENP6 and SENP7 showed lower processing activities compared with deconjugation of SUMO substrates, but in all instances, they show a clear isoform preference for SUMO2/3 (24–27). SENP3 and SENP5 have also been reported to possess an isoform preference for SUMO2/3 (25, 28, 29).

SENP/ULP family members are localized in different regions inside of the cell, most being nuclear. Cellular localization is controlled by the distinct N-terminal extensions of the SENP/ULP family members, and it has been proposed that these regions regulate the activity of the protease. For example, SENP2 is localized to filaments of the nuclear pore complex (30), but differential splicing produces SENP2 protease variants that can shuttle between the cytoplasm and the nucleus (31). SENP3 and SENP5 have been localized in the nucleolus (30). SENP6 and SENP7 are localized in the nucleoplasm, and SENP6 has been recently shown to be implicated in the assembly of the inner kinetochore during mitotic progression (32).

SENP6 and SENP7 are the most divergent members within the SENP/ULP family (5, 25) with a catalytic domain displaying a lower sequence similarity and conserved sequence insertions in distinct loop regions. Biochemical and structural studies of the SENP7 catalytic domain suggested a role for the Loop 1 insertion in the proteolytic activity of the enzyme, whereas Loop 2 and Loop 3 insertions were dispensable (26). In the present study, we have further investigated the structural determinants of Loop 1 insertion in the proteolytic activity of SENP6 and SENP7 and have identified a novel and more extensive interface between SUMO and this subclass of SUMO proteases. Furthermore, we show that the region of SUMO involved in the interface with Loop 1 is responsible for the isoform preference displayed by SENP6 and SENP7 for SUMO2/3. Single point mutagenesis on the SUMO surface allows SENP6 and SENP7 to swap their SUMO2/3 isoform specificity for SUMO1. In conclusion, we disclose a novel and more extended substrate-enzyme interface between SUMO and the SENP6 and SENP7 subclass of SUMO proteases.

EXPERIMENTAL PROCEDURES

Protein Mutagenesis and Purification—The catalytic domains of human SENP2-(364–589), SENP6-(637–1112), and SENP7-(662–984) were produced in *Escherichia coli* and purified as described (19, 26). All SUMO1 and SUMO2 constructs, including precursors, double glycine insertions at the C terminus, and mature forms, were produced in *E. coli* as described before (19, 20). Conjugation and purification of RanGAP1-SUMO substrates were produced as described previously (33).

Single point mutations were introduced into the SUMO1 (A72N, H75D, S9C, and C52S), SUMO2 (N68A, D71H, and K11C) and SENP7 (K691E, K691A) coding regions using the QuikChange mutagenesis kit (Stratagene). The SENP7 four mutant construct P686G/P687G/P688G/P689G was constructed by PCR. PCR was used to construct SENP6 deletion mutants by fusing amino acids 656–664 (Loop-1 SENP6-Δ657–663), substituting two glycine residues for the loop between residues 720 and 735 (Loop 2 SENP6-Δ721–734), and fusing amino acids 874 to 973 (Loop 3 SENP6-Δ875–972) of SENP6 and by fusing amino acids 683–692 (Loop 1 SENP7-Δ682–691) of SENP7. All constructs were confirmed by DNA sequencing. SENP6 deletion mutants were purified by metal affinity chromatography and gel filtration (as described before for SENP7) (26) and concentrated to 1 mg/ml in a buffer containing 25 mM Tris-HCl (pH 8.0), 350 mM NaCl, and 1 mM β-mercaptoethanol.

To prepare the diSUMO2 dimer, Δ14-SUMO2 was produced as SUMO donors, and SUMO2ΔGG (deletion of the C-terminal di-Gly motif) was produced as SUMO acceptor. Both proteins were produced and purified in *E. coli* as described before for the wild type (19). DiSUMO2 was formed overnight at 37 °C in a reaction mixture containing 20 mM HEPES (pH 7.5), 5 mM $MgCl_2$, 0.1% Tween, 50 mM NaCl, 1 mM dithiothreitol, 2 mM ATP, 150 nM SAE1/SAE2 (E1), 100 nM Ubc9 (E2), IR1 (E3), 32 mM Δ14-SUMO2, and 16 mM SUMO2ΔGG in MilliQ water; and purified by gel filtration (Superdex75, GE Healthcare). The diSUMO2(N68A/D71H) double point mutant and diSUMO2(D71K) were prepared as the wild type form, but instead of using Δ14-SUMO2 as the SUMO donor, a triple single point mutant with a deletion of the first eight amino acid residues, Δ8-SUMO2(K11C/N68A/D71H), and Δ14-SUMO2(D71K) were utilized.

Biochemical and Kinetic Assays—Titration of the carboxyl-terminal hydrolase activity (processing) was measured by incubating preSUMO1GGG$_i$G$_i$-*X*, preSUMO1GGG$_i$G$_i$-*X*(A72N/H75D), preSUMO2GGG$_i$G$_i$-*X* and preSUMO2GGG$_i$G$_i$-*X*(N68A/D71H) (-*X* represents the natural C-terminal tail sequence for each SUMO isoform, and G$_i$ represents the glycine insertions) precursor proteins (5 μM) with purified SENP6, SENP7, and SENP2 at three different enzyme concentrations (0.5, 5, and 50 nM) at 37 °C in a buffer containing 25 mM Tris-HCl (pH 8.0), 150 mM NaCl, 0.1% Tween 20, and 2 mM dithiothreitol. Reactions were stopped after 25 min with SDS loading buffer and analyzed by gel electrophoresis (PAGE). Proteins were detected by staining with SYPRO (Bio-Rad).

Identical experimental conditions were used to assay the deconjugation activities for SENP2, SENP6 wild type and deletion mutants, and SENP7 at 0.5, 5, 50 nM using RanGAP1-SUMO1, RanGAP1-SUMO1(A72N/H75D), RanGAP1-SUMO2, and RanGAP1-SUMO2(N68A/D71H) substrates at 3 mM. Deconjugation activities using diSUMO2 substrates at 3 μM were performed using enzyme concentrations at 0.05, 0.5, and 50 nM. For the titration analysis, the reactions were stopped after 25 min with SDS loading buffer and analyzed by PAGE. Proteins were detected by staining with SYPRO (Bio-Rad). Products were quantified by detecting fluorescence under UV illumination using a Gel-Doc apparatus with associated integration software (Quantity One; Bio-Rad).

Processing and deconjugation time course reactions were performed with similar buffer conditions as for the end point reactions. SENP6 and SENP2, at 5 and 1 nM respectively, were incubated with RanGAP1-SUMO1, RanGAP1-SUMO1(A72N/H75D), RanGAP1-SUMO2, and RanGAP1-SUMO2(N68A/D71H) substrates at 3 μM. Reactions were run at 37 °C and stopped at 5, 20, 40, and 80 min with SDS loading buffer and analyzed by PAGE. The same buffer conditions were used for the time course reactions using diSUMO2 and diSUMO2(N68A/D71H) mutant with SENP2, SENP6, and SENP7 at 0.5 nM and diSUMO2 and diSUMO2(D71K) with SENP7, SENP7-ΔLoop 1, SENP7(K691E), SENP7(K691A), and SENP7(P686G/P687G/P688G/P689G) at 0.5 nM with reactions stopped at 15, 30, 60 and 120 min.

Initial reaction velocities were measured for SENP6-ΔLoop 3 at 1 nM and SENP7 and associated mutants at 0.5 nM in a buffer containing 25 mM Tris-HCl (pH 8.0), 150 mM NaCl, 0.1% Tween 20, and 2 mM dithiothreitol at 37 °C. Substrates used for the processing and deconjugation reactions were prepared at 5 μM. Reactions were stopped at indicated time intervals with SDS loading buffer and analyzed by PAGE. Products were quantified by detecting fluorescence using a Gel-Doc apparatus with associated integration software (Quantity One; Bio-Rad). All data points were fitted to a hyperbolic curve. All assays were conducted in triplicate. *Error bars* indicate ±1 S.D.

Michaelis-Menten steady-state kinetics was performed for SENP6 by introduction of S9C and C52A point mutants into SUMO1 and SUMO1(A68N/H71D) to allow for fluorophore addition. SUMO1(S9C/C52C) and SUMO1(S9C/C52C/A68N/H71D) were used for labeling with Alexa Fluor 488 fluorophore (Invitrogen) and were subsequently conjugated to RanGAP1. Initial deconjugation velocities were measured at eight different substrate-labeled concentrations (0, 0.25, 1, 2, 6, 20, 50, and 100 μM) for a SENP6 concentration at 25 nM. Reactions were stopped after 0, 5, 15, 40, and 80 min with SDS loading buffer and analyzed by SDS gel electrophoresis. Fluorescence signal was followed and measured by using Versadoc apparatus with associated integration software (Quantity One, Bio-Rad). Kinetic constants were obtained from the graph representation substrate concentration (μM) *versus* initial velocity (μM min^{-1}). All assays were conducted in triplicate.

RESULTS

Mutagenic Analysis of Loop 1 Insertion in SENP7—In a previous work, we partially characterized the proteolytic activity of the four sequence insertions located in the catalytic domain of SENP7 (named Loop 1 to Loop 4) (26). Of special interest is the Loop 1 insertion, which is composed of eight residues, including four prolines, two glycines, and a lysine residue in the center of the loop (Fig. 1). Loop 1 is structured in the crystal structure of SENP7, and its deletion produced important defects in the proteolytic activity of SENP7 (26). Loop 1 is unique to the SENP6 and SENP7 subclass, and the sequence alignment displays a high degree of sequence identity with respect to SENP6, with only one single amino acid substitution (Thr-690 for Ala) (Fig. 1*C*). A structural feature of Loop 1 is the presence of a short stretch of four proline residues, forming a poly-proline helix structure. A poly-proline helix is a type of secondary structure that restrains conformational flexibility of Loop 1, despite its lack of interactions with the core of the protease.

To determine the structural basis for the Loop 1 role in the proteolytic activity, we designed several mutant constructs of Loop 1 of SENP7. The first construct contained the substitution of the four consecutive prolines residues by glycines. The SENP7 (P686G/P687G/P688G/P689G) mutant will assess the role of Loop 1 in the activity of the protease by disrupting its spatial conformation. The introduction of four glycines increases the flexibility of the main chain of Loop 1 and could lead to a non-productive interaction with the SUMO substrates in activity assays. Loop 1 contains only one prominent charge residue at the center of it, Lys-691, which could be relevant by establishing polar interactions with SUMO substrates. We have designed two single point mutants, Lys-691 to Glu, to invert its charged properties, and Lys-691 to Ala, which removes both the basic ϵ-amino group and the aliphatic side chain.

SENP7 Loop 1 mutants were tested against diSUMO2 and polySUMO2 chains substrates by using time course deconjugation analysis (Fig. 1, *D* and *G*). Deletion of Loop 1 seriously compromises the proteolytic activity of SENP7 as described previously (26). The SENP7 Loop 1 mutant construct of four prolines to glycines (Fig. 1, SENP7, P686G/P687G/P688G/P689G), which would increase the flexibility of Loop 1, reduces the proteolytic activity of SENP7 as much as deletion of the whole Loop 1 does. SENP7 single point mutant of Lys-691 to glutamic acid (SENP7(K691E) in Fig. 1) also dramatically reduces the proteolytic activity of the protease. Finally, the SENP7 single point mutant of Lys-691 to alanine (SENP7(K691A) in Fig. 1) has a reduction of the proteolytic activity to a lesser degree compared with the other constructs. To estimate the differences in the activity, initial rate velocities were measured for the diSUMO2 deconjugation reaction at 0.5 nM of final enzyme concentration (Fig. 1, *E* and *F*). Deconjugation rates for SENP7 wild type are ~10–20-fold faster than SENP7-ΔLoop 1, SENP7(K691E), and SENP7(P686G/P687G/P688G/P689G), whereas for SENP7(K691A), the activity reduction is not so marked compared with the other mutant constructs.

These biochemical analyses with the SENP7 mutant constructs reveal that both the spatial conformation of Loop 1 and the charge properties of Lys-691 are important for a productive interaction of SENP7 with SUMO2 and thus for the correct cleavage of SUMO substrates. It is worth noting that Loop 1 only represents a small region of the total interface of SENP7 and SENP6 with SUMO and that it is not present in the other members of the mammalian SENP family. Loop 1 interaction with SUMO has not been described previously, and our data indicate that it can enhance the proteolytic activity for SENP6 and SENP7. Our next step was to figure out the putative surface region in SUMO that directly interacts with Loop 1 of SENP6 and SENP7.

Loop 1 SENP7 Interaction with SUMO2—Based on previous structures of the complexes of SENP2 with either SUMO1 or SUMO2 (19, 20), we have predicted a region on the SUMO surface that is located close to Loop 1 of SENP6 and SENP7. Crystal structures of the complex between SENP1, SENP2, or ULP1 with SUMO indicate that the main residues involved in

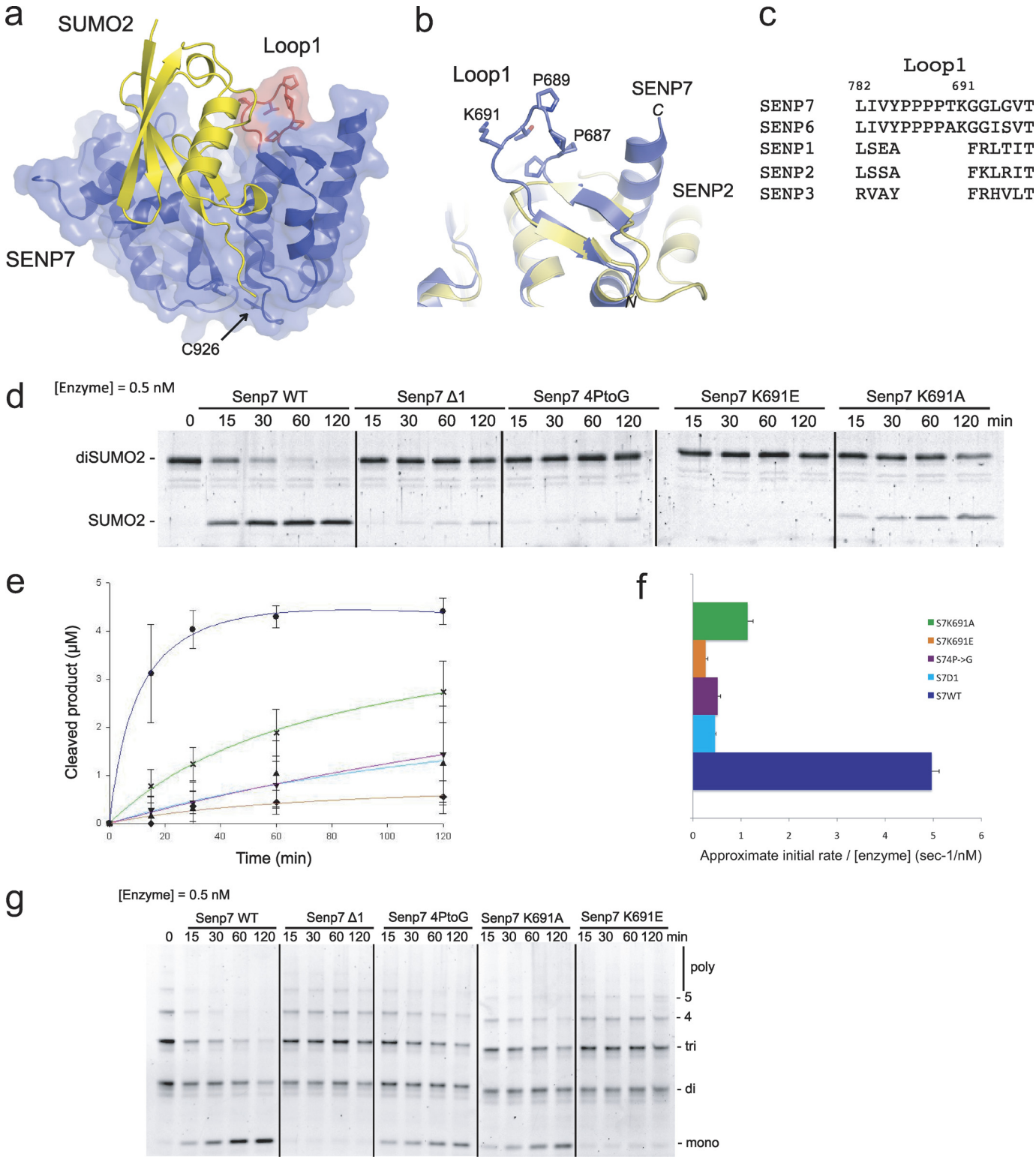

FIGURE 1. **Deconjugation analysis of Loop 1 mutant constructs in SENP7.** *a* and *b*, superposition of SENP2 and SENP7 catalytic domains in *pink* and *blue*, respectively. The position of SUMO2 is indicated schematically based on SUMO2 in complex with SENP2 (Protein Data Bank code 2IO0). SENP7 Loop 1 is indicated in *red* to highlight the relative position in respect to the entire protease. Key residues are highlighted in *stick* representation and labeled accordingly. *c*, sequence alignment of SENP proteases based on structural similarity highlighting Loop 1 insertion in SENP6 and -7. *d* and *g*, deconjugation assays of SENP7 and associated mutants at 0.5 nM enzyme concentration against diSUMO2 and polySUMO2, respectively. Assays were run were run at time intervals indicated above each lane in minutes. *e*, kinetic analysis of deconjugation of diSUMO2 by SENP7 and associated mutants taken at 0, 15, 30, 60, and 120 min. *f*, bar representation of approximate initial rate velocities for deconjugation of diSUMO2 determined within a linear range from data obtained from *e*. *Axes* are labeled, and *error bars* were obtained by conducting assays in triplicate.

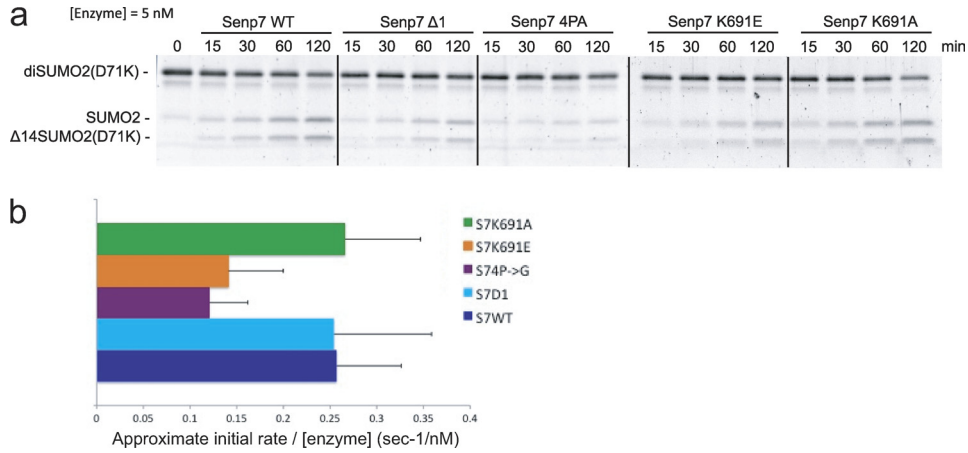

FIGURE 2. **Deconjugation of diSUMO2(D71K) with SENP7 Loop 1 mutant constructs.** *a*, deconjugation assays of SENP7 and associated mutants against diSUMO2(D71K). Assays were run at 5 nM enzyme concentration, and time intervals are indicated *above each lane* in minutes. *b*, bar representation of approximate initial rate velocities for deconjugation of diSUMO2(D71K) determined within a linear range based on data obtained from kinetic analysis taken at 0, 15, 30, 60, and 120 min (not shown). *Axes* are labeled, and *error bars* were obtained by conducting assays in triplicate.

the interface and in the catalysis are conserved for all members of the SENP/ULP protease family. Thus, despite the lack of a crystal structure of the complex, we assume that the extended quilt-like interface observed between SUMO and SENP2 is going to be conserved for the SENP6 and SENP7 complexes. Our structural model indicates that a slight conformational move can place Loop 1 close to a SUMO surface region. This surface seems to be more negatively charged for the SUMO2 isoform compared with SUMO1 (see Fig. 3, *A* and *B*). Thus, the disruption of this interface would be responsible for the SENP7 proteolytic defects described in Fig. 1.

To investigate this region, we have produced a single point mutation in SUMO2 of Asp-71 for lysine, which could interfere with the positive charge created by the side chain of Lys-691 of Loop 1 of SENP7. We were able to synthesize diSUMO2 with SUMO2(D71K) as a substrate for deconjugation assays. Time course proteolytic cleavage of diSUMO2(D71K) substrate shows a decrease in the proteolytic activity for all SENP7 constructs tested, including the wild type form (Fig. 2*A*). Time course deconjugation reactions were run at 5 nM final enzyme concentrations, one order of magnitude higher than the experiments in Fig. 1*D*. Particularly interesting is the loss of proteolytic activity in SENP7 wild type that becomes as defective as all Loop 1 mutant constructs (Fig. 2, *A* and *B*). It is worthwhile to mention that just a single change of charge, Asp-71 for lysine, on the surface of SUMO2 distant from the cleavage site can produce marked defects in the proteolytic activity of SENP7, with an approximately loss of 20-fold with respect to the diSUMO2 wild type reaction (see supplemental Fig. 1). These results support the formation of this novel and more extended interface between Loop 1 and SUMO2.

Deconjugation Analysis of SUMO Isoform Preference for SENP6 and SENP7—Different groups have reported a preferential proteolytic activity of SENP6 and SENP7 subclass for SUMO2/3 isoform (25–29, 34). We have predicted a novel interface involving Loop 1, unique to the SENP6 and SENP7 subclass, and SUMO, with different residues involved depending on the SUMO isoform type. We already showed that the Loop 1 interaction improves the catalytic activity for SENP6 and SENP7, and our next assessment was to check whether Loop 1 also had a role for the SUMO2/3 isoform preference. Based on a model of the complex between SENP7 and SUMO2, we analyzed the chemical nature of the residues of SUMO1 and SUMO2/3 in contact with Loop 1 of SENP7. We observed that the SUMO2/3 amino acid residues involved in the interface have a more polar nature when compared with the analogous SUMO1 residues, more specifically, Asp-71 (His in SUMO1) and Asn-68 (Ala in SUMO1) (Fig. 3, *A* and *B*). We wanted to investigate whether these residues could account for the SUMO2/3 isoform preference showed by SENP6 and SENP7 (26).

To test our hypothesis, we first produced SUMO2 with two point mutations, Asn-68 for Ala and Asp-71 for His, making a version of SUMO2 that resembles the SUMO1 interface with Loop 1 of SENP7. Similarly, we also produced SUMO1 with equivalent single point mutation positions used for SUMO2 double point mutant to revert the trend of the proteolytic reaction. Double point mutant SUMO2(N68A/D71H) and SUMO1(A72N/H75D) behaved similarly to wild type SUMO1 or SUMO2 during gel filtration and anion exchange purification, indicating that the two SUMO double mutants did not appear to present a barrier to protein folding. We also conjugated SUMO2(N68A/D71H) and SUMO1(A72N/H75D) to RanGAP1 to generate the canonical model substrate used in our deconjugation assays. The conjugation of double point SUMO mutants to RanGAP1 behaved similarly to the conjugation of wild type SUMO1 and SUMO2 (data not shown).

SENP6, SENP7, and SENP2 were first compared in deconjugation assays using wild type and double point mutants as substrates, namely RanGAP1-SUMO1, RanGAP1-SUMO2, RanGAP1-SUMO1(A72N/H75D), and RanGAP1-SUMO2(N68A/D71H) (Fig. 3*C*). Three different enzyme concentrations were used in the titration assays (0.5, 5, and 50 nM) in the presence of 3 μM of each RanGAP1-SUMO substrate. As observed in Fig. 3*C*, SENP2 is more active and does not discriminate between wild type and double point mutants of SUMO1 and SUMO2. However, in the case of SENP6, there is a noticeable reduction of activity for the SUMO2 double point mutant and an increase of activity for SUMO1 double point mutant. For SENP7, the

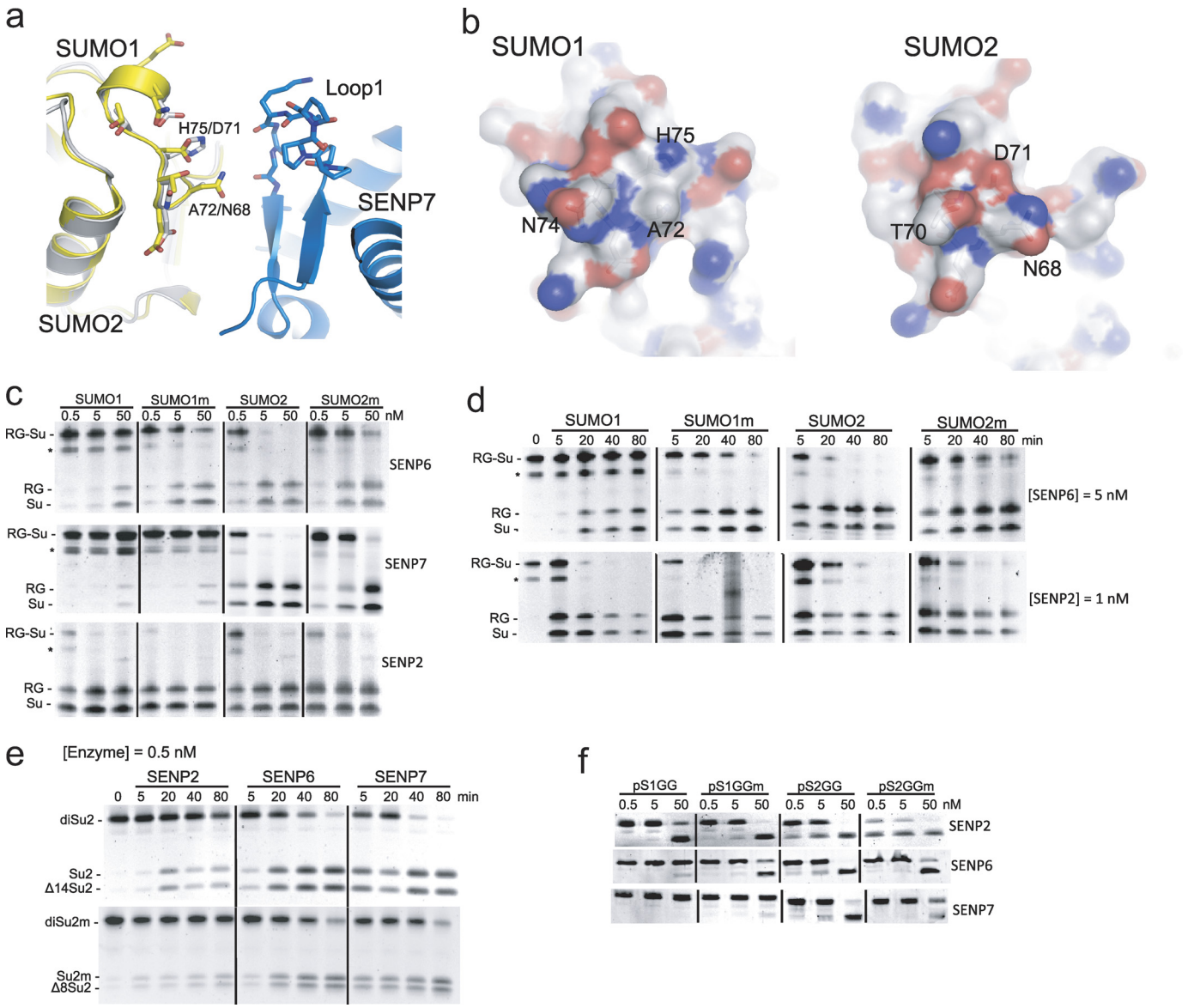

FIGURE 3. **SENP7-SUMO interaction models, processing and deconjugation activites of SUMO isoform mutants.** *a*, structural model of potential interaction sites between SENP7 (*blue ribbon*) and SUMO1 (*gray ribbon*) and SUMO2 (*yellow ribbon*). The positions of SUMO1 and SUMO2 are based on SUMO1 and -2 in complex with SENP2 (Protein Data Bank codes 1THZ and 2IO0). Key residues in the SUMO-protease interface are indicated in *stick* representation and labeled according to their position and side chain composition in both SUMO and SENP7. *b*, electrostatic potential surface representation of SUMO1 and -2 to highlight differences within SENP7 Loop-1 possible interaction sites. All images were modified and represented using the respective Protein Data Bank codes in PyMOL (36). *c* and *d*, activity and time course assays, respectively, of deconjugation of SENP2, SENP6, and SENP7 against RanGAP1-SUMO1 (*RG-Su*), RanGAP1-SUMO1(A72N/H75D), RanGAP1-SUMO2, and RanGAP1-SUMO2(N68A/D71H). An *asterisk* indicates RanGAP1-SUMO degradation products. *e*, time course assay of deconjugation of SENP2, -6, and -7 against diSUMO2 (*diSu2*) and diSUMO2(N68A/D71H) (*diSu2m*). *f*, activity assay of processing of preSUMO1GGG$_i$G$_i$-*X*, preSUMO1GGG$_i$G$_i$-*X* (A72N/H75D), preSUMO2GGG$_i$G$_i$-*X*, and preSUMO2GGG$_i$G$_i$-*X*(N68A/D71H). Activity assays were run at 0.5, 5, and 50 nM enzyme concentration against 5 μM substrate concentration at 37 °C and stopped after 25 min with SDS loading buffer and analyzed via PAGE. Time course assays were run at 0.5 nM enzyme concentration, and time intervals are indicated *above each lane* in minutes. Proteins were detected by staining with SYPRO (Bio-Rad).

decrease in the activity of SUMO2 double point mutant is also appreciated, whereas for SUMO1 no activity is detected, as reported previously by different groups (28–29, 34). These differences are better appreciated in a time course deconjugation reaction, where all RanGAP1-SUMO constructs were substrates in pulse-chased reactions with either SENP2 at 1 nM or SENP6 at 5 nM (Fig. 3*D*). Time course results with SENP6 confirmed the reduction of proteolytic activity for RanGAP1-SUMO2(N68A/D71H) and the increase of activity for RanGAP1-SUMO1(A72N/H75D). In contrast SENP2, despite having a proteolytic activity one order of magnitude faster than SENP6, showed basically no differences between the wild type substrates and the double point mutants. As mentioned above, SENP2 does not contain the Loop 1 insertion in its sequence; thus, the unaltered SENP2 activities between SUMO isoforms could be explained by the lack of the interface between Loop 1 and SUMO.

As stated previously (25–27), SENP6 shows a low degree of proteolytic activity against SUMO1 substrates, in contrast to SUMO2/3, which is preferentially cleaved by the SENP6 and SENP7 family members. Interestingly, a gain of the SENP6 proteolytic activity with RanGAP1-SUMO1(A72N/H75D) com-

pared with RanGAP1-SUMO1 wild type is totally opposed to the loss of activity observed for RanGAP1-SUMO2(N68A/D71H) double point mutant (Fig. 3, *C* and *D*). SENP6 proteolytic activity against RanGAP1-SUMO1(A72N/H75D) is almost as efficient as with RanGAP1-SUMO2 wild type substrate, a striking result for a protease with a reported isoform preference for SUMO2/3 substrates. Thus, in addition to the enhancement of the proteolytic activity in the SENP6 and SENP7 subclass, the unique Loop 1 insertion has a prominent role in the discrimination between the two SUMO isoforms by these proteases.

SENP6 and SENP7 have been suggested to posses a major proteolytic activity for deconjugation of poly-SUMO2 chain substrates (24, 26), with an improved hydrolysis of the isopeptidic bond formed between SUMO2 Lys-11 and the C-terminal Gly-93 from the next SUMO2. We have designed a version of diSUMO2 where the donor SUMO2 contains the two mutations (N68A/D71H) and the acceptor SUMO2 contains a deletion of the C-terminal di-glycine motif to keep off poly-SUMO chain formation. In Fig. 3*E*, a time course deconjugation analysis has been run using SENP2, SENP6, and SENP7 at 0.5 nM. A trend similar to the RanGAP1-SUMO substrates is observed, and the differences between the proteolytic activity for diSUMO2 and diSUMO2(N68A/D71H) are also noticeable, with an activity reduction for the double point mutant of diSUMO2 for SENP6 and SENP7.

Processing Analysis of SUMO Isoform Preference for SENP6 and SENP7—Some groups have reported that the SENP6 and SENP7 subclass displayed poor proteolytic activities in the formation of the mature form of SUMO from their precursors (25–27). However, as described previously (26), addition of two glycine residues after the Gly-Gly motif improved maturation rates substantially for SENP7, minimizing the inhibitory effect of the C-terminal tail observed in the processing reaction (19). Thus, the substrates tested in the processing reactions were preSUMO1GGG$_i$G$_i$-*X*, preSUMO1GGG$_i$G$_i$-*X*(A72N/H75D), preSUMO2GGG$_i$G$_i$-*X*, and preSUMO2GGG$_i$G$_i$-*X*(N68A/D71H). (-*X* represents the natural C-terminal tail sequence for each SUMO isoform, and G$_i$ represents the glycine insertions.) Although the processing is not as efficient as the deconjugation reaction, differences between the wild type forms and the double point mutants can be appreciated in the titration analysis for SENP6 and SENP7 (Fig. 3*F*). A gain of proteolytic activity is observed for the maturation of the SUMO1 double point mutant precursor and a corresponding loss of activity for the SUMO2 double point mutant precursor, compared with their wild type forms. These results support the formation of similar enzyme-substrate complexes between SENP6 and SENP7 with the precursor forms of SUMO1 and SUMO2, and as observed for the deconjugation reaction, a prominent role for the Loop 1 insertion is observed. Interestingly, as observed in the deconjugation reactions, the processing activity for the maturation of SUMO1 precursor in SENP7 is much lower compared with SENP6, as previously stated (25, 26, 34).

SENP6 Loop-insertion Deletion Mutants—To further characterize the catalytic domain of SENP6, we produced three different constructs of SENP6 lacking the equivalent loop insertion sequences observed in the crystal structure of SENP7 (26), namely SENP6-ΔLoop 1, SENP6-ΔLoop 2, and SENP6-ΔLoop 3 (see "Experimental Procedures" for further sequence details). The amino acid sequence of Loop 1 from SENP6 is identical to the corresponding Loop 1 from SENP7, whereas for Loop 2 and Loop 3, the amino acid sequences between SENP6 and SENP7 are not homologous. Interestingly, SENP6 Loop 3 is ~150 residues long compared with SENP7 Loop 3, which is only 50 residues long. In the SENP7 crystal structure, Loop 2 and Loop 3 were disordered, and their removal did not produce any change in the proteolytic activity for all the substrates tested, in contrast to the SENP7 Loop 1 (Fig. 1).

We tested all SENP6 deletion mutants with our canonical model substrates, RanGAP1-SUMO (including the wild type and the double point mutant). In the titration analysis shown in Fig. 4*A* and supplemental Fig. 2, the SENP6-ΔLoop 1 mutant displays a loss of activity for all substrates under these conditions, whereas SENP6-ΔLoop 2 and SENP6-ΔLoop 3 mutants show a similar or higher activity with respect to the wild type form (compare with Fig. 3*C*). Particularly interesting is the increase in the proteolytic activity observed for the SENP6-ΔLoop 3 deletion mutant, which was not observed for SENP7 (26). This gain of proteolytic activity by deleting Loop 3 of SENP6 might be explained by a decrease in the total entropy of the system by removing an insertion of 150 amino acid residues, which is presumably not ordered in the SENP6 structure and could interfere in the correct binding of the substrate.

SENP6 deletion mutants were also run against RanGAP-SUMO1 and RanGAP-SUMO2 double point mutant substrates (Fig. 4*A*). SENP6-ΔLoop 2 and SENP6-ΔLoop 3 deletion mutants show the same trend in the proteolytic activity with the SUMO double point mutant substrates as observed for the SENP6 wild type form (Fig. 3), with an increase and a decrease in the proteolytic activity for SUMO1 and SUMO2 double point mutant, respectively. As stated before, the SENP6-ΔLoop 1 deletion mutant showed a reduced proteolytic activity with either the wild type or any of the double point mutant substrates tested. These results with SENP6 correlate well with the deletion mutant results for SENP7 (26), and support the role of the Loop 1 insertion in the enhancement of the proteolytic activity by the formation of an extended interface with SUMO.

Initial Rate Measurements for SENP6-ΔLoop 3 Mutant—To obtain a more quantitative assessment for the proteolytic differences between the SUMO substrates, initial rate velocities were measured using SENP6-ΔLoop 3 as the protease in both processing and deconjugation reactions. The SENP6-ΔLoop 3 deletion mutant was chosen due to the higher activity level compared with the wild type SENP6, as observed in Fig. 4*A*. Deconjugation assays were pulse chased up to 80 min using RanGAP1-SUMO1, RanGAP1-SUMO1(A72N/H75D), RanGAP1-SUMO2, and RanGAP1-SUMO2(N68A/D71H) substrates. Similarly, processing reactions were analyzed using preSUMO1GGG$_i$G$_i$-*X*, preSUMO1GGG$_i$G$_i$-*X*(A72N/H75D), preSUMO2GGG$_i$G$_i$-*X*, and preSUMO2GGG$_i$G$_i$-*X*(N68A/D71H) substrates (Fig. 4*B*). The enzyme concentration for the deconjugation and processing reaction was 1 and 5 nM, respectively. Enzyme concentrations were optimized in each instance to better estimate the initial rate velocities for each proteolytic reaction.

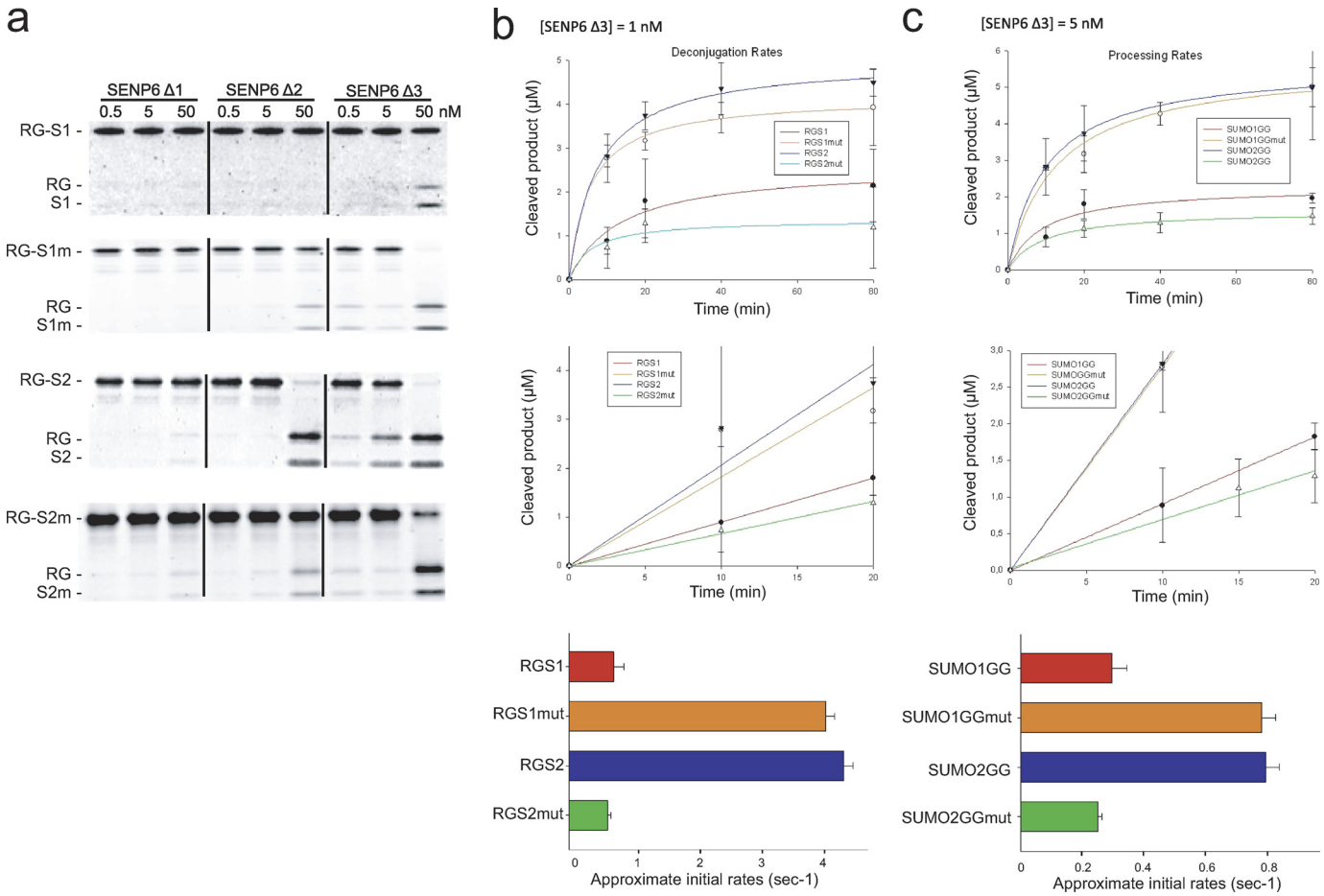

FIGURE 4. **Kinetic analysis for processing and deconjugation of SENP6 deletion mutants.** *a*, deconjugation reaction of RanGAP-SUMO1, RanGAP1-SUMO1(A72N/H75D), RanGAP1-SUMO2, and RanGAP1-SUMO2(N68A/D71H) by SENP6-ΔLoop 1, -ΔLoop 2, and -ΔLoop 3. Activity assays were run at 0.5, 5, and 50 nM enzyme concentration against 5 μM substrate concentration at 37 °C and stopped after 25 min with SDS loading buffer and analyzed via PAGE. Proteins were detected by staining with SYPRO (Bio-Rad). *b* and *c*, deconjugation and processing activity, respectively, of SENP6-ΔLoop 3, were taken at 0, 10, 20, 40, and 80 min; deconjugation and processing initial rate activity of SENP6-ΔLoop 3 were taken at 0, 10, 15, and 20 min; bar representation of initial rate velocities for deconjugation and processing of SENP6-ΔLoop 3 were determined within a linear range from data obtained from *b*. *Axes* are labeled, and *error bars* were obtained by conducting assays in triplicate.

As observed in Fig. 4*B*, the SUMO1(A72N/H75D) double point mutant increases the proteolytic activity of SENP6-ΔLoop 3 by an approximate order of 3- and 5-fold in both processing and deconjugation reactions, respectively. In contrast, the SUMO2(N68A/D71H) double point mutant decreases its proteolytic activity by an order of 4- and 6-fold in the processing and deconjugation reaction, with respect to the wild type SUMO2. Interestingly, the initial rates velocities measured for the SUMO1(A72N/H75D) double point mutant are quite similar to the initial rates velocities displayed by the SUMO2 wild type. These results confirm our previous data and indicate that the SUMO isoform preference displayed by SENP6 for SUMO2/3 can be modulated by swapping two single amino acid residues between SUMO1 and SUMO2/3.

Steady-state Kinetic Analysis of SUMO1 Mutants—To estimate the kinetic parameters of the contribution of this novel surface of SUMO to the proteolytic activity of SENP6 and SENP7 subclass, we developed a more quantitative activity assay using deconjugation substrates that are chemically modified with a fluorophore (Alexa Fluor 488). The maleimide group of Alexa Fluor 488 reacts covalently with cysteine residues. To develop this reagent we have produced a double mutant of SUMO1 with the substitutions of Ser-9 for cysteine and Cys-52 for alanine. SUMO1 (S9C/C52A) is modified with the fluorophore at the flexible N-terminal tail at position 9, which is not essential for activity. Although SUMO1 contains a cysteine residue buried in the hydrophobic core (Cys-52), it has been replaced by alanine to avoid a potential modification by the fluorophore that could affect the catalytic properties of the SUMO proteases. SUMO1 (S9C/C52A) was tested in conjugation assays and compared with SUMO1 wild type to assess that they both have similar catalytic properties (data not shown).

Deconjugation time-course reactions were run using fluorogenic RanGAP1-SUMO1 and RanGAP1-SUMO1(A72N/H75D) substrates with SENP2 and SENP6 at 1 and 25 nM, respectively (Fig. 5). As shown in previous results (Figs. 3 and 4), there is a clear gain of proteolytic activity for the SUMO1(A72N/H75D) double point mutant compared with SUMO1 wild type for SENP6, in contrast to SENP2 where the proteolytic activities for both substrates displayed only minor differences. A Michaelis-Menten representation of the initial velocities measured for a range of substrate concentration varying from 0.25 to 100 μM, displayed hyperbolic curves that allowed us to estimate the catalytic constants of the reaction (Fig. 5, *B* and *C*). Michaelis-Menten

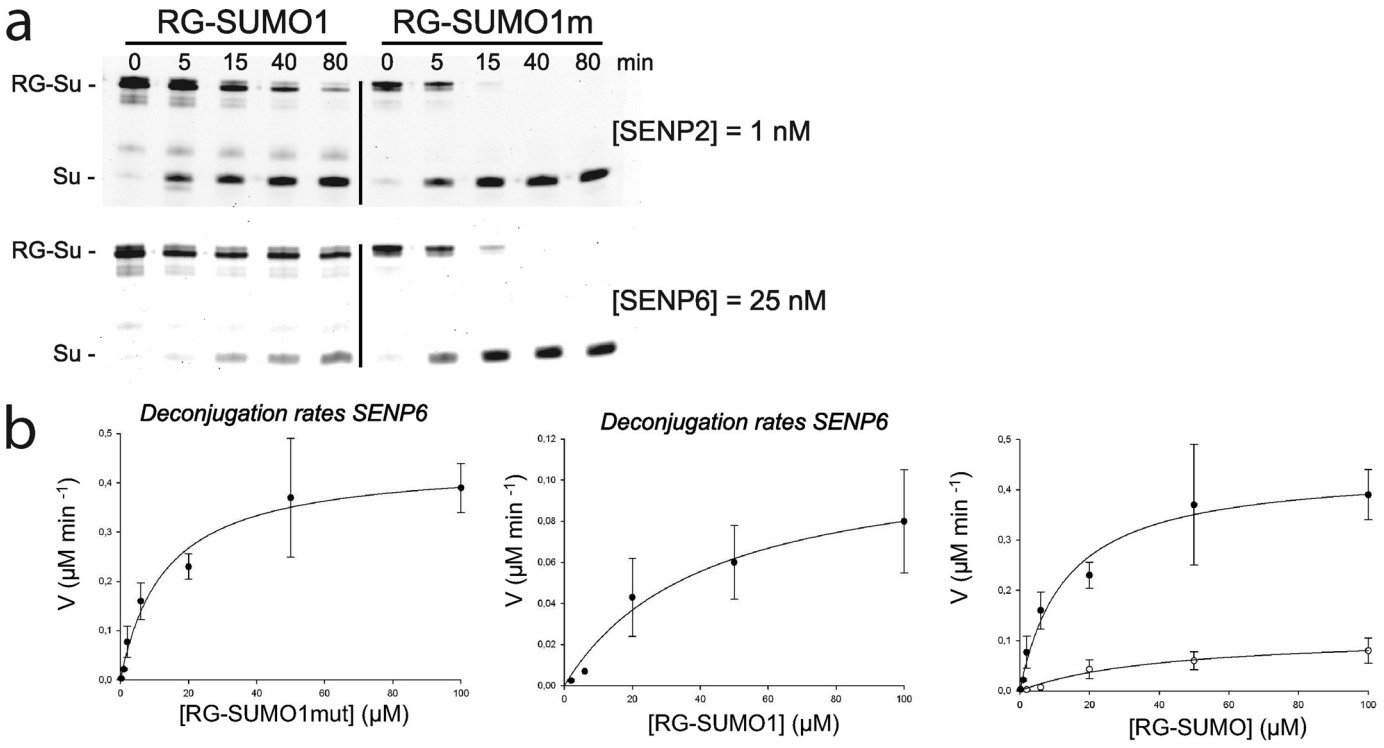

c

	RG-SUMO1mut	*RG-SUMO1*
K_M (μM)	13.16	41.6
k_{cat} (s^{-1})	0.294	0.075
k_{cat} / K_M (M^{-1} s^{-1})	2.25 x 10^4	1.80 x 10^3

FIGURE 5. **Steady-state kinetics of the deconjugation reaction for RanGAP1-SUMO1 and RanGAP1-SUMO1mut by SENP6.** a, Deconjugation activity against RanGAP1-SUMO1 and RanGAP1-SUMO1(A72N/H75D) (*RG-SUMO1m*) with SENP6 and SENP2 at 25 and 1 nM concentrations, respectively. Both substrates are labeled with Alexa Fluor 488, and the kinetics was followed with a VersaDoc apparatus (Bio-Rad). *b*, Michaelis-Menten graphic representation of substrate concentration (μM) *versus* velocity (μM min^{-1}) at time intervals 0, 5, 15, 40, and 80 min for RanGAP1-SUMO1mut (*left*) and RanGAP1-SUMO1 (*middle*). *The right panel* depicts a comparison of the two graphs. Initial rate deconjugation activities were measured at five different substrate concentrations (0, 0.25, 1, 2, 6, 20, 50, and 100 μM) and at 25 nM SENP6 concentration. Reactions were stopped after intervals indicated above each lane in minutes with SDS loading buffer and analyzed by gel electrophoresis. *c*, table of the kinetic coefficients K_m, k_{cat}, and k_{cat}/K_m obtained from data in b for RanGAP1-SUMO1 and RanGAP1-SUMO1mut.

constants K_m were 41.6 and 13.16 μM for SUMO1 and SUMO1(A72N/H75D) substrates, respectively; whereas the catalytic constant k_{cat} were 0.075 and 0.294 s^{-1} for SUMO1 and SUMO1(A72N/H75D) substrates, respectively. The total gain of proteolytic activity by the SUMO1 double point mutant is ~12.5-fold, as estimated by the k_{cat}/K_m catalytic efficiency of the enzyme. Based on these results, this novel interface between Loop 1 of SENP6 and SENP7 and SUMO affects both the binding and the catalytic properties of the enzyme.

DISCUSSION

SENP6 and SENP7, the most divergent SUMO proteases of the SENP/ULP family with respect to the catalytic domain, contain sequence insertions in the catalytic domain whose removal compromises the proteolytic activity of the enzyme. In particular, deletion of the Loop 1 insertion in SENP6 and SENP7 results in a diminished activity in both processing and deconjugation reactions, whereas deletion of Loop 2 and Loop 3 display similar or even higher activities with respect to the wild type form (as observed for SENP6-ΔLoop 3). Biochemical and mutagenesis analysis on Loop 1 insertion reveal that both the structural conformation of the loop and the charge properties of the side chain of Lys-691 are basic for the correct proteolytic activities showed in the SENP7 reactions. In particular, the putative interaction with the SUMO surface of the ϵ-amino group of Lys-691 seems fundamental for a correct formation of the enzyme-substrate complex, and this interaction seems only to occur with a particular structural conformation of Loop 1. This property is restricted to SENP6 and SENP7 family members, because for the other members of the SENP/ULP family, the Loop 1 sequence is not present, and at least for SENP1 and SENP2, this lack of sequence does not suppose a constraint for their proteolytic activity (19, 21, 25, 34). Thus, we predict a more extended interface for SENP6 and SENP7 in the complex with SUMO, including the Loop 1 insertion present only in this subclass of SUMO proteases.

Several groups have reported that SENP6 and SENP7 preferred SUMO2/3 as substrates in deconjugation and processing reactions (25–27). The specificity of the SENP family members for the different SUMO isoforms is largely based on contacts at

the interface of the SENP and SUMO structures. A structural model based on the crystal structure of the interaction of SENP2 with SUMO2 suggests a region of SUMO that could interact with the Loop 1 of SENP7. In particular, in our model, the locations of residues Asp-71 and Asn-68 in the structure of SUMO2 are in a short contact distance with Loop 1 of SENP7, presumably by establishing polar interactions. Substitution of these residues by the corresponding SUMO1 residues histidine and alanine, respectively, reduce the protease activity for all of the substrates tested. Interestingly, when we swap the corresponding SUMO1 residues with residues from SUMO2, a notable gain of proteolytic activity can be observed for all SUMO1 substrates tested, and in some instances becomes as active as with the SUMO2 substrate and thus reverts the isoform preference of SENP6 and SENP7.

This novel SUMO interface is only relevant for the SENP6 and SENP7 family members because these are the only SUMO proteases with a Loop 1 insertion in their catalytic domains. For the other members of the SENP/ULP protease family, SENP3 and SENP5 have also been reported to have a strong selectivity for SUMO2/3, but in this case, a different region in the SUMO surface may account for such activity. However, we cannot rule out the possibility of the formation of a similar Loop 1 structure due to the lack of structural information for SENP3 and SENP5 catalytic domains. This is in contrast to SENP1 and SENP2 catalytic domains, where SUMO isoform differences for the deconjugation reaction are minor (19, 21). In the SUMO maturation reaction, it has been reported that the two residues in the C-terminal tail immediately following the cleavage site were responsible for the SENP1 and SENP2 isoform preference (19, 21, 35). A recent study confirmed the different SUMO isoform specificities shown in the human SENP/ULP family by using SUMO-vinyl sulfone adducts for *in vivo* experiments and SUMO-amidomethyl coumarin as substrates (34). In this study, a similar SUMO2/3 isoform preference for the SENP6 and SENP7 catalytic domains is confirmed, and interestingly, it is suggested that the N-terminal domain of some SUMO proteases can influence their paralog specificity (34).

The SENP6 and SENP7 subclass of the SENP/ULP family are the most divergent with respect to their catalytic domain. In this study, we have identified a region in the SUMO surface that is responsible for the SUMO isoform preference for SUMO2/3 displayed by this subclass of SUMO proteases. Single point mutagenesis in this region can swap their SUMO isoform preference between SUMO2/3 and SUMO1. The disclosure of this region reveals important insights into the biochemical and structural biology of the SUMO deconjugation reaction, and it can lead to the development of valuable tools for studying the SUMO isoform specificity inside of the cell. Although additional structural work will be required to describe in detail the physical basis of this novel SUMO-SENP interface, our biochemical and mutagenesis experiments suggest how SENP6 and SENP7 are able to discern between SUMO1 and SUMO2/3 isoforms.

Acknowledgment—We acknowledge Christopher D. Lima for reagents and support.

REFERENCES

1. Hershko, A., and Ciechanover, A. (1998) *Ann. Rev. Biochem.* **67,** 425–479
2. Kerscher, O., Felberbaum, R., and Hochstrasser, M. (2006) *Annu. Rev. Cell Dev. Biol.* **22,** 159–180
3. Geiss-Friedlander, R., and Melchior, F. (2007) *Nat. Rev. Mol. Cell Biol.* **8,** 947–956
4. Johnson E. S. (2004) *Annu. Rev. Biochem.* **73,** 355–382
5. Mukhopadhyay, D., and Dasso, M. (2007) *Trends Biochem. Sci.* **32,** 286–295
6. Owerbach, D. A., McKay, E. M., Yeh, E. T., Gabbay, K. M., and Bohren, K. M. (2005) *Biochem. Biophys. Res. Commun.* **337,** 517–520
7. Vertegaal, A. C., Andersen, J. S., Ogg, S. C., Hay, R. T., Mann, M., and Lamond, A. I. (2006) *Mol. Cell. Proteomics* **5,** 2298–2310
8. Ayaydin, F., and Dasso, M. (2004) *Mol. Biol. Cell* **15,** 5208–5218
9. Gareau, J., and Lima, C. D. (2011) *Nat. Rev. Mol. Cell Biol.* **12,** 861–871
10. Bossis, G., and Melchior, F. (2006) *Mol. Cell* **21,** 349–357
11. Knipscheer, P., and Sixma, T. A. (2003) *Curr. Opin. Struct. Biol.* **6,** 665–673
12. Matic, I., van Hagen, M., Schimmel, J., Macek, B., Ogg, S. C., Tatham, M. H., Hay, R. T., Lamond, A. I., Mann, M., and Vertegaal, A. C. (2008) *Mol. Cell Proteomics* **7,** 132–144
13. Tatham, M. H., Jaffray, E., Vaughan, O. A., Desterro, J. M., Botting, C. H., Naismith, J. H., and Hay, R. T. (2001) *J. Biol. Chem.* **276,** 35368–35374
14. Fu, C., Ahmed, K., Ding, H., Ding, X., Lan, J., Yang, Z., Miao, Y., Zhu, Y., Shi, Y., Zhu, J., Huang, H., and Yao, X. (2005) *Oncogene* **24,** 5401–5413
15. Tatham, M. H., Geoffroy, M. C., Shen, L., Plechanovova, A., Hattersley, N., Jaffray, E. G., Palvimo, J. J., and Hay, R. T. (2008) *Nat. Cell Biol.* **10,** 538–546
16. Békés, M., Prudden, J., Srikumar, T., Raught, B., Boddy, M. N., Salvesen, G. S. (2011) *J. Biol. Chem.* **286,** 10238–10247
17. Lallemand-Breitenbach, V., Jeanne, M., Benhenda, S., Nasr, R., Lei, M., Peres, L., Zhou, J., Zhu, J., Raught, B., and de Thé, H. (2008) *Nat. Cell Biol.* **10,** 547–555
18. Mossessova, E., and Lima, C. D. (2000) *Mol. Cell* **5,** 865–876
19. Reverter, D., and Lima, C. D. (2004) *Structure* **12,** 1519–1531
20. Reverter, D., and Lima, C. D. (2006) *Nat. Struct. Mol. Biol.* **13,** 1060–1068
21. Shen, L. N., Dong, C., Liu, H., Naismith, J. H., and Hay R. T. (2006) *Biochem. J.* **397,** 279–288
22. Shen, L., Tatham, M. H., Dong, C., Zagórska, A., Naismith, J. H., and Hay, R. T. (2006) *Nat. Struct. Mol. Biol.* **13,** 1069–1077
23. Xu, Z., Chau, S. F., Lam, K. H., Chan, H. Y., Ng, T. B., and Au, S. W. (2006) *Biochem. J.* **398,** 345–352
24. Mukhopadhyay, D., Ayaydin, F., Kolli, N., Tan, S. H., Anan, T., Kametaka, A., Azuma, Y., Wilkinson, K. D., and Dasso, M. (2006) *J. Cell Biol.* **174,** 939–949
25. Mikolajczyk, J., Drag, M., Békés, M., Cao, J. T., Ronai, Z., and Salvesen, G. S. (2007) *J. Biol. Chem.* **282,** 26217–26224
26. Lima, C. D., and Reverter, D. (2008) *J. Biol. Chem.* **283,** 32045–32055
27. Shen, L. N., Geoffroy, M. C., Jaffray, E. G., and Hay, R. T. (2009) *Biochem. J.* **421,** 223–230
28. Di Bacco, A., Ouyang, J., Lee, H. Y., Catic, A., Ploegh, H., and Gill, G. (2006) *Mol. Cell. Biol.* **26,** 4489–4498
29. Gong, L., and Yeh, E. T. (2006) *J. Biol. Chem.* **281,** 15869–15877
30. Zhang, H., Saitoh, H., and Matunis, M. J. (2002) *Mol. Cell. Biol.* **22,** 6498–6508
31. Itahana, Y., Yeh, E. T., and Zhang, Y. (2006) *Mol. Cell. Biol.* **26,** 4675–4689
32. Mukhopadhyay, D., Arnaoutov, A., and Dasso, M. (2010) *J. Cell Biol.* **188,** 681–692
33. Reverter, D., and Lima, C. D. (2009) *Methods Mol. Biol.* **497,** 225–239
34. Kolli, N., Mikolajczyk, J., Drag, M., Mukhopadhyay, D., Moffatt, N., Dasso, M., Salvesen, G., and Wilkinson, K. D. (2010) *Biochem. J.* **430,** 335–344
35. Xu, Z., and Au, S. W. (2005) *Biochem. J.* **386,** 325–530
36. DeLano, W. L. (2010) *The PyMOL Molecular Graphics System*, version 0_99rc6, Schrödinger, LLC, New York